Shape coexistence in ^{180}Hg studied through the β decay of ^{180}Tl

J. Elseviers,[1] A. N. Andreyev,[1,2] S. Antalic,[3] A. Barzakh,[4] N. Bree,[1] T. E. Cocolios,[1,5] V. F. Comas,[6] J. Diriken,[1] D. Fedorov,[4] V. N. Fedosseyev,[7] S. Franchoo,[8] J. A. Heredia,[6] M. Huyse,[1] O. Ivanov,[1] U. Köster,[9] B. A. Marsh,[7] R. D. Page,[10] N. Patronis,[1,11] M. Seliverstov,[1,5] I. Tsekhanovich,[12] P. Van den Bergh,[1] J. Van De Walle,[5] P. Van Duppen,[1] M. Venhart,[1,13] S. Vermote,[14] M. Veselský,[13] and C. Wagemans[14]

[1]*Instituut voor Kern- en Stralingsfysica, K.U. Leuven, University of Leuven, BE-3001 Leuven, Belgium*
[2]*School of Engineering and Science, University of the West of Scotland, Paisley, PA1 2BE, UK and the Scottish Universities Physics Alliance (SUPA)*
[3]*Department of Nuclear Physics and Biophysics, Comenius University, SK-84248 Bratislava, Slovakia*
[4]*Petersburg Nuclear Physics Institute, RU-188350 Gatchina, Russia*
[5]*ISOLDE,CERN, CH-1211 Geneve 23, Switzerland*
[6]*Gesellschaft für Schwerionenforschung, Planckstrasse 1, DE-64291 Darmstadt, Germany*
[7]*EN Department, CERN, CH-1211 Geneve 23, Switzerland*
[8]*Institut de Physique Nucléaire, IN2P3-CNRS/Université Paris-Sud, FR-91406 Orsay Cedex, France*
[9]*Institut Laue Langevin, 6 rue Jules Horowitz, FR-38042 Grenoble Cedex 9*
[10]*Department of Physics, Oliver Lodge Laboratory, University of Liverpool, Liverpool L69 7ZE, UK*
[11]*Department of Physics, University of Ioannina, GR-45110 Ioannina, Greece*
[12]*CENBG, CNRS IN2P3, Univ. Bordeaux I, FR-33175 Gradignan, France*
[13]*Slovak Academy of Sciences, SK-84511 Bratislava, Slovakia*
[14]*Department of Physics and Astronomy, University of Gent, Proeftuinstraat 86, BE-9000 Gent, Belgium*

(Received 23 June 2011; published 7 September 2011)

The β^+/EC decay of ^{180}Tl and excited states in the daughter nucleus ^{180}Hg have been investigated at the CERN On-Line Isotope Mass Separator (ISOLDE) facility. Many new low-lying energy levels were observed in ^{180}Hg, of which the most significant are the 0_2^+ at 419.6 keV and the 2_2^+ at 601.3 keV. The former is the bandhead of an excited band in ^{180}Hg assumed originally to be of prolate nature. From the β feeding to the different states in ^{180}Hg, the ground-state spin of ^{180}Tl was deduced to be $(4^-,5^-)$.

DOI: 10.1103/PhysRevC.84.034307 PACS number(s): 21.10.Re, 23.20.Lv, 27.70.+q, 29.38.−c

I. INTRODUCTION

Even-even mercury isotopes have been found to be a prolific testing ground for the phenomenon of shape coexistence [1–3], whereby different types of deformation coexist at low excitation energy within the same nucleus. Shape coexistence in the neutron-deficient mercury nuclei has been observed by using different techniques, ranging from optical [4] and laser spectroscopy [5,6] to in-beam spectroscopy [7,8] and decay spectroscopy [9,10]. A wealth of new data has become available recently through lifetime measurements [11,12] and by using new techniques such as Coulomb excitation of postaccelerated radioactive beams [13].

The excitation energies of the yrast-band members of the even-even mercury isotopes between $A = 190$ and 198 (see Fig. 1) show an almost constant behavior and are believed to be associated with the weakly deformed oblate ground state ($\beta_2 \sim -0.15$). This pattern is distorted in the lighter mercury isotopes through the intrusion of a strongly deformed prolate band ($\beta_2 \sim 0.25$) as discussed in Ref. [2,3]. This band is built on top of a deformed excited 0_2^+ state, which is interpreted as resulting from proton excitations across the $Z = 82$ closed shell [14]. Such intruder states have been found to be a widely occurring structural feature of nuclei at and near closed shells. The emerging picture for intruder-state behavior in mercury isotopes is the parabolic trend of the excitation energy of states in the prolate band as a function of the neutron number N. Studies of the lightest even-even isotopes $^{174-180}$Hg [3,15–18] showed that the minimum of the energy of the intruder structure was probably reached in ^{182}Hg ($N = 102$), although the 0_2^+ bandhead had not been observed in ^{180}Hg before the present work. Also the 2_2^+ state in ^{180}Hg was not firmly established; a state at 797 keV was proposed in Ref. [18] as the 2^+ member of the prolate band, but this is not validated in the present study.

Furthermore, theoretical predictions [14] suggest a transition from a weakly oblate to a spherical ground state of the even-even mercury isotopes with $N < 96$. Indeed, the observed evolution of the ground-state band properties, i.e., the high excitation energy of the first 2^+ and 4^+ states in ^{174,176}Hg [3] supports this prediction.

Shape coexistence is not the only reason to study ^{180}Tl decay. The main aim of the present experiment was the study of the β-delayed fission of ^{180}Tl [19]. To investigate the β-delayed fission probability, the β branching ratio of ^{180}Tl has to be known precisely. This can be determined by investigating the β decay of ^{180}Tl. Furthermore, the heavier odd-odd thallium isotopes with $A = 188$–196 have typically two β-decaying isomers [20]. If ^{180}Tl has also more than one β-decaying isomer, it is important to know through which isomer the β-delayed fission occurs. The existence of isomerism in ^{180}Tl could possibly be verified via a β-γ study.

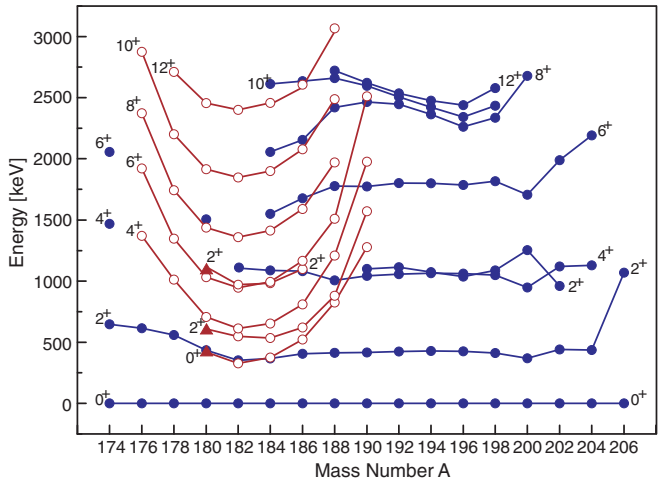

FIG. 1. (Color online) Energy systematics of excited states of even-even neutron-deficient mercury isotopes. The energies are taken from Refs. [3,12,20–22]. The filled triangles show the states identified in this work. The full dots are the level energies associated with the weakly oblate ground-state band, the open dots are those related to the excited prolate band. However, at low spin states, strong mixing can occur [23].

The present paper reports on the results of an experiment carried out to study low-lying excited states of ^{180}Hg through the EC/β^+ decay of ^{180}Tl. Prior to this study, the states of ^{180}Hg had only been investigated by using the technique of in-beam γ-ray spectroscopy in conjunction with the recoil-decay tagging technique [11,12,17,18]. These experiments show three excited bands, up to spin $I = (22)$. In contrast with in-beam spectroscopy, which predominantly reveals yrast states, the β-decay spectroscopy allows deeper insight into low-lying nonyrast coexisting states.

II. EXPERIMENTAL SETUP

The experiment was performed at the CERN On-Line Isotope Mass Separator (ISOLDE) facility [24] and is part of a systematic α, β, and β-delayed fission study of neutron-deficient thallium isotopes. Protons from the CERN Proton Synchrotron (PS) booster, with an energy of 1.4 GeV and an average intensity of 2.1 μA, impinged on a 50 g cm^{-2} UC$_x$ target, producing a wide variety of nuclei through fission, spallation, or fragmentation. The thallium isotopes were predominantly formed through spallation. The proton beam consisted of pulses that had a length of 2.4 μs and a period of 1.2 s. During the experiment, a sequence of 21 pulses was grouped into a so-called supercycle with a total length of 25.2 s. The amount of proton pulses that ISOLDE received changed throughout the experiment from four to ten pulses per supercycle.

After the proton impact, the produced radioactive isotopes diffused across and effused from the target material toward an ion source through a heated transfer line. To reduce the release time, the target-ion source was kept at a high temperature of $\approx$ 2300 K. The desired thallium isotopes were subsequently ionized with the resonant laser ionization technique [25]. The ionized thallium isotopes were extracted from the target-ion source using extraction electrodes and were accelerated to 30 keV. The High Resolution Separator [26] was used to separate the isotopes according to their mass to charge ratio. As a result, a high-purity beam of ^{180}Tl nuclei was obtained. By comparing the ratio of the number of thallium nuclei in spectra taken with the lasers tuned to the ionization of thallium to spectra taken without lasers, a fraction of only 1.4(1)% of surface-ionized ^{180}Tl was observed.

The decay of ^{180}Tl was observed using the so-called Windmill system [19]. After mass separation, the incident thallium beam of $\sim$ 150 atoms/s was implanted in one of ten 20 μg cm^{-2} thick carbon foils mounted on a wheel. Any long-living radioactivity was removed from the implantation position by rotating the wheel after every supercycle. The proton pulses of the supercycle were chosen in such a way that two consecutive proton pulses were taken followed by a period without proton pulses (see Fig. 2). The separator gate was opened from the moment the first proton pulse arrived until 1.2 s after the second proton pulse.

Two Si detectors were placed at the implantation position in close geometry. An annular detector having an active area of 450 mm^2, thickness of 300 μm and a central hole with a diameter of 6 mm was positioned in front of the foil, so that the ion beam could pass through its hole. A circular detector of active area 300 mm^2 and thickness 300 μm was placed behind the foil. Both detectors together covered a solid angle of 66% of 4π. The energy resolution (full width at half maximum, FWHM) of these detectors for α decays in the range of 5000–7000 keV was $\sim$ 35 keV. As the primary aim of these experiments was the detection of β-delayed fission, the energy range was set to 200 keV to 100 MeV to record events from electrons, positrons, α particles, and fission fragments. Outside the vacuum chamber, at $\sim$2 cm from the implantation point, a Miniball Ge cluster detector was placed, which consisted

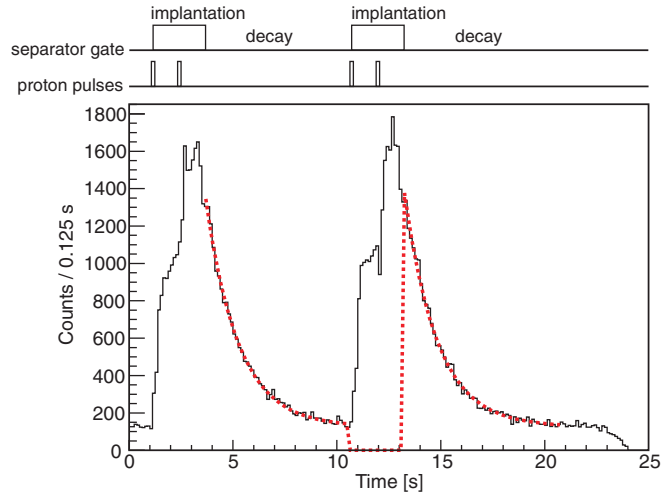

FIG. 2. (Color online) Time behavior for the $2_1^+ \rightarrow 0_1^+$ (434 keV) transition in ^{180}Hg as a function of the implantation and decay periods within one supercycle, defined by the proton pulses and the separator gate, which determines the implantation period. The red dotted line is the exponential fit of the "decay" intervals.

of three high-purity germanium (HPGe) crystals [27]. The typical energy resolution (FWHM) of each crystal of the cluster for 1.3 MeV γ radiation was ∼3.1 keV. The absolute photo-peak efficiency of the whole cluster for the 434 keV line, the strongest transition in ^{180}Hg, was determined to be 7.3(1)%. The $\gamma\gamma$ coincidences used in the analysis of the experiment were those between the three crystals of the cluster. In the detection setup, digital electronics [digital gamma finder (DGF) modules [28]] were used to acquire the data.

III. RESULTS

The half-life of ^{180}Tl can be determined from its α decay or β-delayed γ decay. The α-decay spectrum can be found in Ref. [19] and the time behavior after β decay is illustrated in Fig. 2, which shows the time behavior for the $2_1^+ \rightarrow 0_1^+$ (434 keV) transition in ^{180}Hg. The half-life of ^{180}Tl was determined by fitting the "decay" intervals between proton implantations with an exponential (see Fig. 2). This results in a half-life of $t_{1/2} = 1.09(1)$ s for the α and β decay of ^{180}Tl. Except for several unresolved and/or weak lines, most of the γ transitions attributed to ^{180}Hg (see Table I) have a time behavior that within uncertainty is consistent with this half-life. Although isomerism is observed in the heavier thallium isotopes, no evidence for the presence of an isomer could be extracted from the half-life behavior of ^{180}Tl β-delayed γ decays.

A β branching ratio of 94(4)% for ^{180}Tl was determined from a comparison of the number of α and β decays (for more details, see Ref. [19]).

Figure 3 shows a γ-ray energy spectrum measured at $A = 180$ with the Miniball Ge cluster, in which transitions belonging to the decay of ^{180}Tl are indicated. The assignment of γ lines to the β decay of ^{180}Tl is based on $\gamma\gamma$ coincidences and on previously known transitions in ^{180}Hg [17,18]. Other strong lines in Fig. 3 that do not originate from the decay of ^{180}Tl come from the decay of beam contaminants. These mainly consist of ^{38,39,40}Cl, ^{140,142}La, and ^{141,142}Ba. It is believed that molecules of mass 180 are formed between the chlorine isotopes and the barium or lanthanum isotopes, which are not fully suppressed by the High Resolution Separator. One of the strongest lines in the spectrum is the 511 keV γ ray, originating mainly from the annihilation of the positron resulting from the β^+ decay of ^{180}Tl or from pair production of high-energy γ rays.

An example of a $\gamma\gamma$ coincidence spectrum is shown in Fig. 4, with a coincidence gate on the strongest transition in ^{180}Hg, namely, the 434 keV ($2_1^+ \rightarrow 0_1^+$) transition. In this spectrum, the background is subtracted by also taking $\gamma\gamma$ coincidence spectra with a gate on the left and right hand sides of the 434 keV peak in the energy spectrum, and normalizing to the peak-to-background ratio. This method results in the appearance of artificial peaks (denoted as AP in the figure) in the $\gamma\gamma$ coincidence spectrum. The two artificial peaks in Fig. 4 are due to the strong peaks at 827 and 1460 keV in the γ-ray energy spectrum, Fig. 3. This is due to Compton scattering between the crystals of the Miniball Ge cluster. Due to this Compton scattering, these artificial peaks are broader than

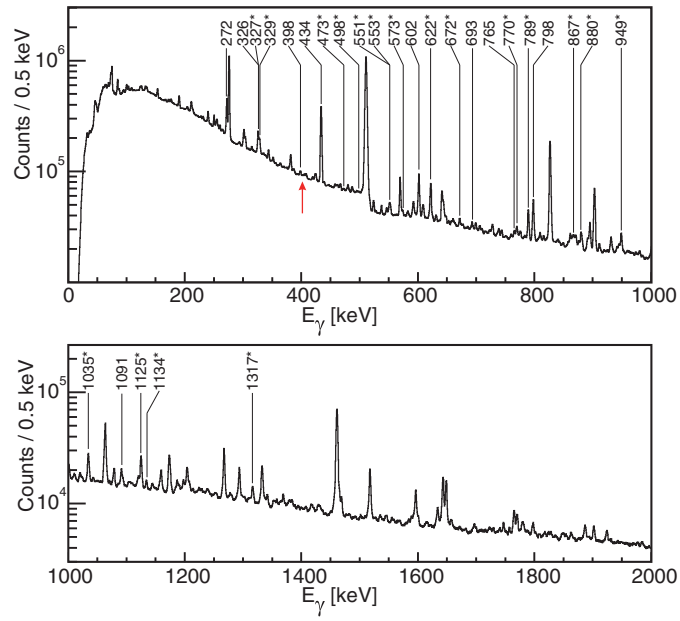

FIG. 3. (Color online) A γ-ray energy spectrum detected by the Miniball Ge cluster for mass 180. Transitions associated with the decay of ^{180}Tl are indicated (energies are in keV). New transitions, which were observed for the first time in the present study, are shown with *. Note that the 405 keV γ ray (indicated by the red arrow) that deexcites the known 8^+ state in ^{180}Hg [18] is not observed. The other lines are due to room background and through the presence in the $A = 180$ beam of molecules with mass 180 (see text for details).

real transitions and they can be identified in the background-subtracted $\gamma\gamma$ coincidence spectrum by the large drops on the the left and right side of the artificial peak.

Table I gives the energy and γ intensity, relative to the 434 keV transition, of all the transitions in ^{180}Hg identified in the present study, as well as the energy of the initial state and the γ rays with which the specific transition is coincident. Due to the close distance of the Miniball Ge cluster to the implantation point, summing between γ rays in a cascade can occur. Note that no correction for this summing was made in the determination of the γ intensities. The resulting level scheme of ^{180}Hg is shown in Fig. 5. The spins of the levels at

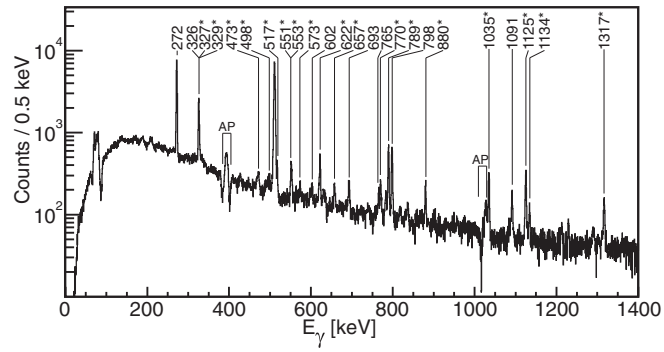

FIG. 4. A $\gamma\gamma$ coincidence spectrum with gate on the 434 keV transition. AP stands for artificial peak, see text for details. New transitions are indicated by * and γ-ray energies are in keV.

TABLE I. Energy, γ-ray intensity (without correction for summing) relative to the transition at 434 keV, energy of the initial state, and observed coincident γ rays for the transitions belonging to the decay of ^{180}Tl. The γ-ray intensities are determined from the γ-ray singles spectrum, unless otherwise indicated. Due to the occurrence of doublets and triplets, a number of observed coincident γ rays could not be uniquely assigned to one particular transition and are therefore grouped and indicated by curly brace. New transitions, observed for the first time in the present study, are marked by an asterisk.

Energy[a] (keV)	Relative γ intensity (%)	Initial energy level (keV)	Observed coincident γ rays (keV)
104.7*	1.4(4)[b]	706.0	
167.0*	3.3(2)	601.3	
181.8*	0.16(1)[c]	601.3	
272.0	54.2(27)	706.0	326, 398, 434, 472, 498, 518, 574, 693, 765, 798, 1091, 1125, 1134 1317, 1456, 1782
325.8	15.3(10)[d]	1031.8	{ 272, 434, 473, 552, 602, 621, 765, 790, 798,
326.8*	5.6(9)[d]	2348.4	{ 1035, 1317, 1455
328.6*	2.7(17)[d]	1797.1	
398.2	2.9(2)	1797.1	272, 551, 602, 693, 798
434.0	100	434.0	167, 272, 326, 472, 498, 518, 552, 574, 602, 622, 658, 693, 765, 770, 790, 798, 880, 949, 1035, 1091, 1125, 1134, 1229, 1456, 1781
472.5*	1.1(2)	1504.2	272, 326, 434
498.1*	1.3(2)[d]	1203.8	272, 434
517.4*	3.4(4)[d]	1223.4	272, 434, 798, 1125
551.1*	3.0(4)[d]	2348.4	{ 327, 398, 434, 573, 602, 622, 765, 867, 1035,
553.0*	2.9(4)[d]	2021.8	{ 1091
573.4*	1.6(2)	1797.1	434, 517, 551, 602, 622, 790
601.6	24.3(12)[d]	601.3	{ 327, 398, 434, 552, 573, 602, 622, 636, 798,
602.4*	1.5(2)[d]	1203.8	{ 867, 949, 1125
622.0*	18.5(9)	1223.4	327, 434, 551, 574, 602, 798, 1125
657.3*	1.0(2)	1091.3	434, 773
671.6*	0.79(4)[e]	1091.3	773
692.9	2.4(2)	1399.0	272, 398, 434, 949
765.4	1.5(1)	1797.1	272, 326, 434, 551
769.7*	3.5(2)	1203.8	434, 635
789.4*	10.4(12)	1223.4	327, 434, 551, 573, 798, 1125
797.7	4.5(17)[d]	1399.0	{272, 327, 398, 434, 518, 602, 622, 789, 949
798.0	5.1(18)[d]	1504.2	
798.1*	9.2(6)[d]	2021.8	
867.1*	1.9(2)[d]	1468.5	434, 552, 602, 880
880.3*	5.0(4)	2348.4	434, 602, 867, 1035
948.9*	3.5(11)[d]	2348.4	272, 434, 602, 693, 798
1034.6*	7.5(8)	1468.5	327, 434, 553, 880
1091.2	2.3(1)	1797.1	272, 434, 551
1125.1*	9.7(5)	2348.4	272, 434, 518, 602, 622, 790
1134.2*	1.1(1)[d]	1840.0	272, 434
1228.9*	0.8(2)[d]	1662.9	434
1316.5*	3.9(2)	2021.8	272, 326, 434, 602
1455.4*	0.6(1)[d]	2487.4	272, 325, 434
1781.5*	1.6(3)[d]	2487.4	272, 434

[a]The uncertainty on the energies is 0.2 keV for the strong transitions; for the weak transitions ($I_\gamma \leqslant 1.5\%$), the error can rise up to 0.5 keV.
[b]Calculated from the intensity of the 272 keV transition, the relative branching ratio of the 272 keV and the 105 keV transition (89% and 11%, respectively, determined from $\gamma\gamma$ coincidences) and the theoretical total $E2$ conversion coefficient of the 105 keV transition (4.575 according to Ref. [30]).
[c]Determined from the γ spectrum with a gate on the K electron of the $E0$ transition between the first two 0^+ states (see Fig. 9).
[d]Determined from $\gamma\gamma$ coincidences.
[e]Determined from the number of $E0$ transitions observed and the efficiency to detect conversion electrons.

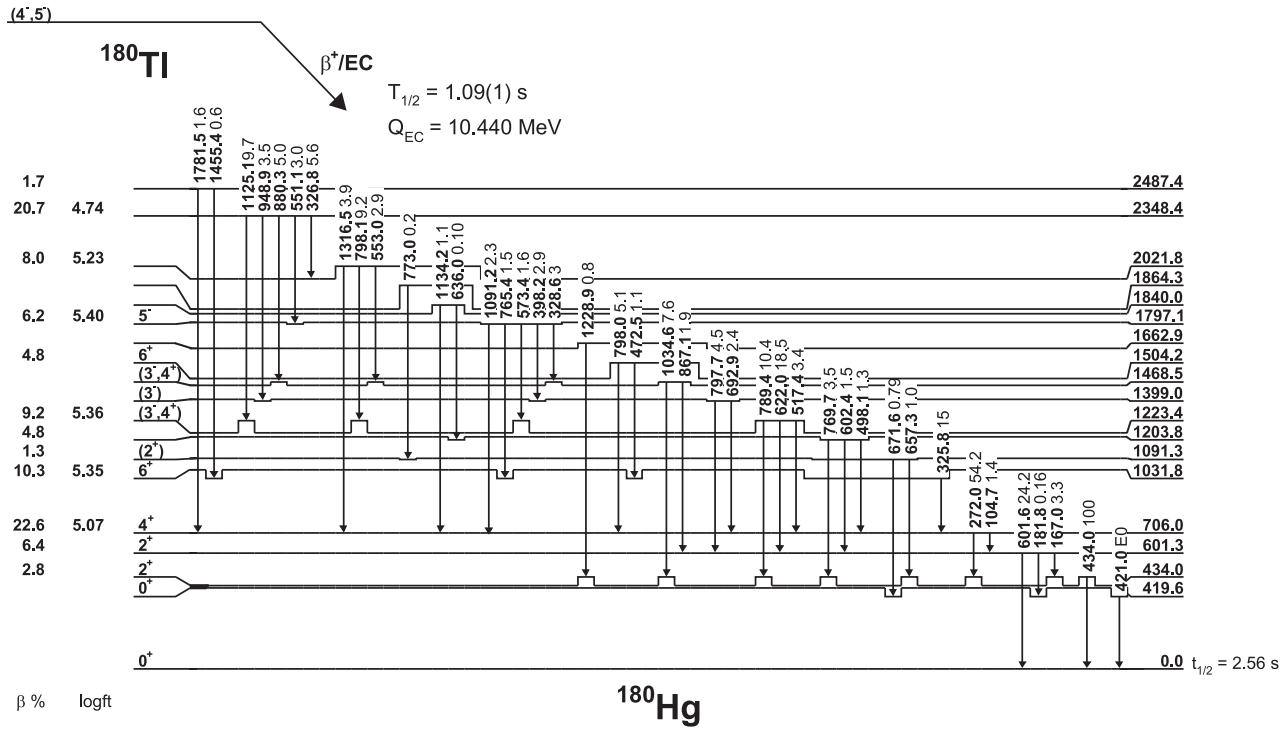

FIG. 5. Level scheme of ^{180}Hg deduced from the present work. γ-ray intensities are all normalized to the 434 keV transition (energies in keV). The given β-feeding intensities are upper limits. The calculated Q_{EC} value is taken from Ref. [29].

434 keV (2^+), 706 keV (4^+), 1032 keV (6^+), 1399 keV (3^-), 1504 keV (6^+), and 1797 keV (5^-) are taken from Ref. [18]. Note that the known 8^+ level at 1437 keV, deexciting with a 405 keV γ line [18] is not observed in this decay study. The β-feeding intensities are based on the intensities from Table I using the internal conversion coefficients for transitions where the multipolarity is known. The internal conversion coefficients are taken from Ref. [30]. However, due to the pandemonium effect [31], only upper limits of the β-feeding intensities can be given. From the β-feeding intensities and the Q_{EC} value to a specific level, the $\log ft$ values can be deduced. Only the $\log ft$ values for the energy levels with the strongest β-feeding intensities are given, because these will not change significantly, even if there is some unobserved γ-ray feeding.

Many new states have been observed in ^{180}Hg, of which the most significant are the 0_2^+ (420 keV) and the 2_2^+ (601 keV) states. The latter differs from the one suggested by Kondev *et al.* [18], namely, a 2_2^+ state at 797.3 keV. In the current study, the 798 keV transition is placed on top of the 601 keV transition, and not vice versa as proposed in Ref. [18]. Our assignment is based on unambiguous coincidence relations. The 601 keV state is a 2^+ state, since the 167 keV transition to the first excited 2^+ at 434 keV has an important $E0$ component. This is clear from investigating the $\gamma\gamma$ coincidence spectrum, with a gate on the 622 keV transition (see Fig. 6), which is placed on top of the 601 keV state in the ^{180}Hg level scheme. This transition is coincident with both the 602 and 434 keV lines. From these coincidences the total relative intensity of the 167 keV transition between the 601 and the 434 keV states could be deduced by comparing the number of counts in the 602 and 434 keV peaks in this coincidence spectrum. This gave a total relative intensity of $I_{tot} = 15(1)\%$, which is much larger than the observed relative γ intensity of this transition $I_\gamma = 3.3(2)\%$. From this the total internal conversion coefficient of the 167 keV transition $\alpha = 3.5(4)$ was deduced, indicating that this transition is dominated by a strong $E0$ component, as the theoretical total electron conversion coefficients for a 167 keV $M1$ and $E2$ transition are 1.83 and 0.74, respectively [30].

The 0_2^+ state at 420 keV has been identified by investigating Si-γ coincidences. Due to the limited thickness of the Si

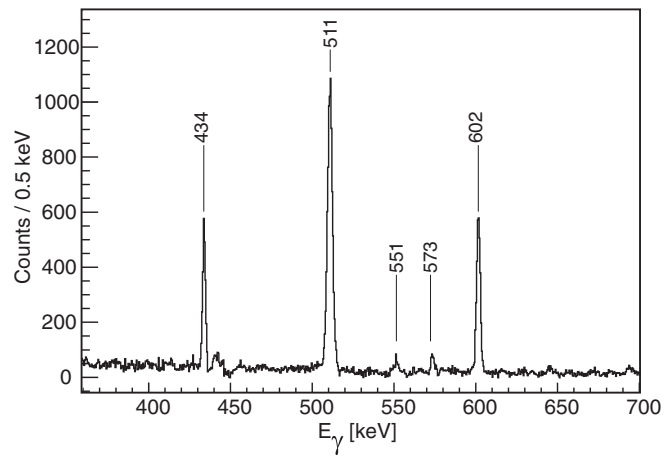

FIG. 6. Part of the $\gamma\gamma$ coincidence spectrum with a gate on the 622 keV transition (energies in keV).

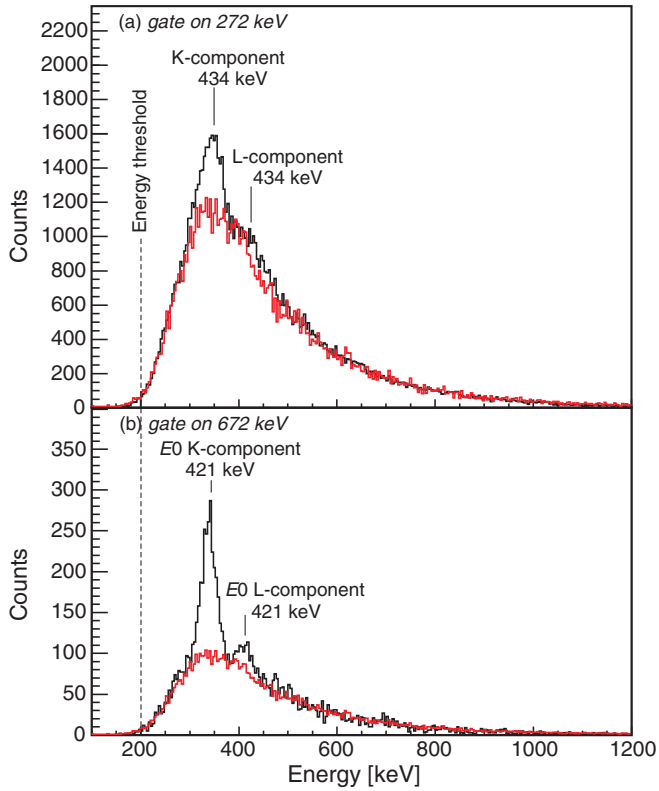

FIG. 7. (Color online) Si spectrum gated on (a) the 272 keV and (b) the 671 keV transition. The red lower curve is the ΔE spectrum due to β particles (see text for details).

detectors (300 μm), they mainly acted as ΔE detectors for electrons and positrons coming from the β decay yielding a ΔE peak around $\sim$ 120 keV. However, due to the energy threshold, the efficiency dropped for electron energies below 400 keV to become zero around 200 keV [see Fig. 7(a)]. By gating on the $2_1^+ \rightarrow 0_1^+$ 434 keV, the $4_1^+ \rightarrow 2_1^+$ 272 keV, and the $6_1^+ \rightarrow 4_1^+$ 326 keV γ-ray transitions, for which the conversion coefficients ($E2$ transitions) and the K- and L-electron energies are known, energy and efficiency calibrations for the Si detectors in the energy range between 300 and 500 keV was performed. This is illustrated in Fig. 7(a), which shows the Si spectrum with a gate on the 272 keV transition.

In this figure, the background due to β particles, which is actually the ΔE spectrum of the β particles, is shown by the red lower curve. This background was deduced from Si spectra taken in a range between 5 and 11 s after the second proton pulse (see Fig. 2). These spectra are dominated by β decay of the daughter nuclei of ^{180}Tl because most of the ^{180}Tl has decayed away. The β background is normalized with the gated Si spectra in the energy range between 500 and 1000 keV. The $E0$ transition of the hitherto unobserved 0^+ prolate bandhead is expected in the range of 300 to 500 keV. By inspecting the γ rays coincident with electrons and positrons in this energy range, a new transition appeared at 672 keV (see Figs. 8 and 3). This transition does not belong to any of the daughter products of ^{180}Tl or to any of the known contaminants and is coincident with mercury x rays.

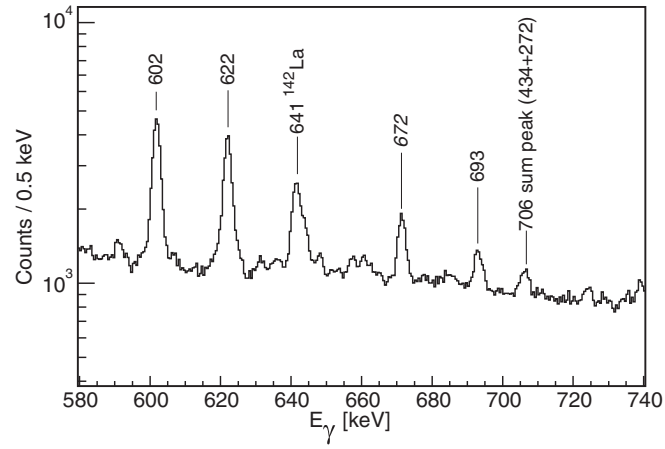

FIG. 8. Part of the γ spectrum with a gate on the Si events that have an energy between 200 and 1200 keV (energies in keV).

By looking at the events in the Si detector which are coincident with the 672 keV transition, a strong peak appears, see Fig. 7(b). This is interpreted as the K-electron peak of the $E0$ transition between the 0_2^+ state and the ground state, placing the former at 421(20) keV. The fact that no γ rays of 421 keV are observed confirms that this is the 0_2^+ state. A small peak due to the electrons from all the other $E0$ ($L, M, N, \ldots$) components can also be seen, indicated in the figure as the L component, because this is the strongest of these transitions. The K-to-total ratio was deduced from this figure as $K/\text{tot} = 0.85(18)$. This is consistent with the value for an $E0$ transition determined in Ref. [30] ($K/\text{tot} = 0.8543$), but other multipolarities cannot be excluded with the current precision.

Furthermore, in Fig. 9 part of the background-subtracted γ-ray spectrum with a gate on the K-electron energy of the $E0$ transition is shown. Next to mercury K x rays a new γ transition appears at 182 keV, which is equal, within error bars, to the difference between the 2_2^+ state and the 0_2^+ state. In this figure the 272 keV transition also appears. This is due to the fact that the K-electron energies of the internal conversion of the

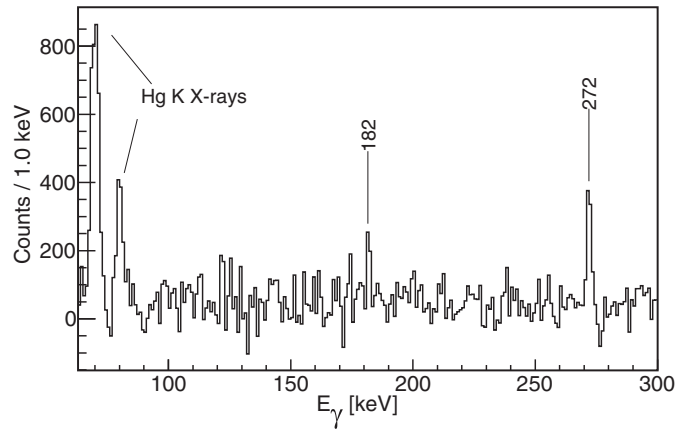

FIG. 9. Part of the background-subtracted γ spectrum with gate on the K electron of the $E0$ transition between the first two 0^+ states (energies in keV).

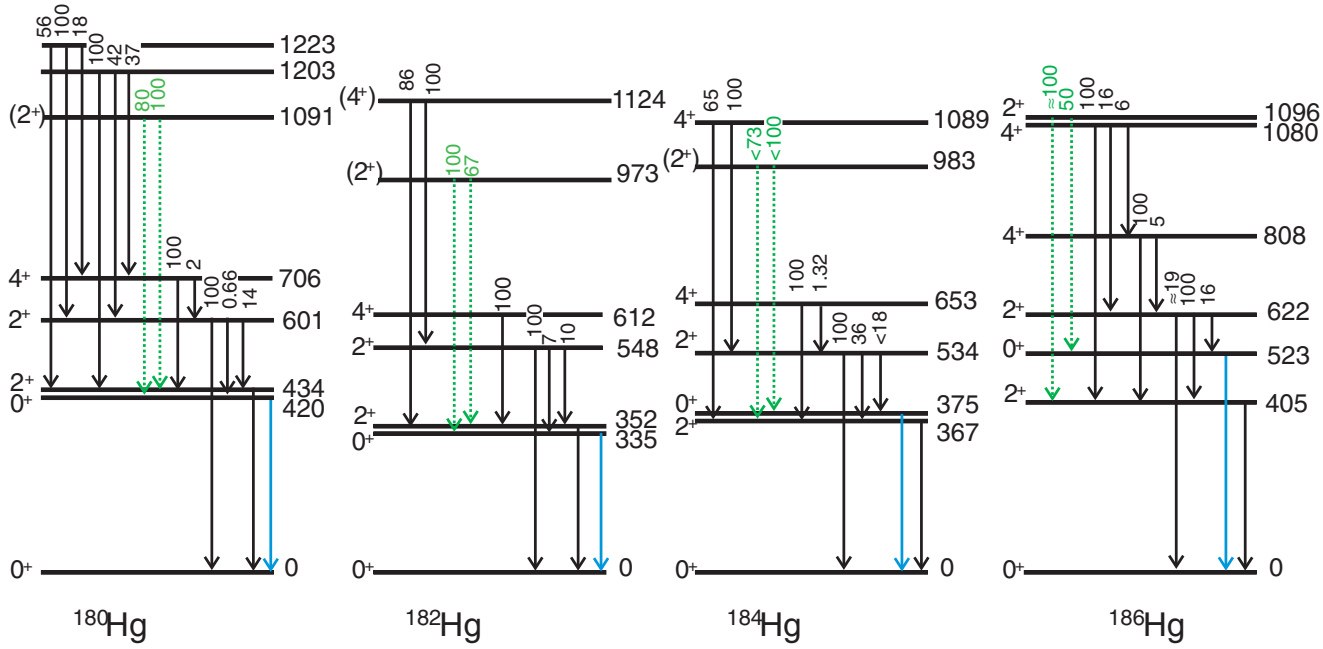

FIG. 10. (Color online) Systematics of the lowest positive-parity states and their transitions in the even-even $^{182-186}$Hg nuclei. The green dotted lines are the γ-ray transitions of the possible γ-vibrational bandhead, i.e., the 2_3^+ state (see text for details). The relative γ-ray intensities are taken from the present work and Refs. [20,22] and level energies are given in keV.

434 keV transition and of the 420 keV transition are very close in energy. Finally, connecting γ rays and coincidence relations with the 672 and 182 keV transitions fixes the energy of the 0_2^+ state at 419.6(4) keV and leads to the identification of the states at 1091 and 1864 keV. Other new levels that have been observed are 1204, 1223, 1469, 1663, 1840, 2022, 2348, and 2487 keV. A unique spin assignment could not be deduced for any of these states.

We also note that an independent in-beam conversion electron study of ^{180}Hg, using the SACRED spectrometer coupled to the gas-filled recoil separator recoil ion transport unit (RITU) at the University of Jyväskylä [32], observed conversion electrons that corroborate our assumption of the conversion of the $2_2^+ \rightarrow 2_1^+$ 167 keV transition, and the study also observed a 420 keV electron line, giving evidence that the 0_2^+ level is placed at the correct energy (see Fig. 2 of Ref. [32]).

IV. DISCUSSION

A. Ground state of ^{180}Tl

The β feeding of the different states of ^{180}Hg was calculated (see Fig. 5) and used to deduce the most probable ground-state spin of ^{180}Tl, because β decay mainly populates states with a spin differing by $\Delta I = 0, 1$. The heavier odd-odd thallium isotopes from $A = 184$ up to $A = 196$ are characterized by isomerism with two β-decaying states based on the coupling of the $3s_{1/2}$ proton with a $3p_{3/2}$ neutron, leading to a 2^- state, or with a $1i_{13/2}$ neutron leading to a 7^+ state. In ^{180}Tl with $N = 99$, however, the $1h_{9/2}$ neutron orbital has to be considered, leading to some differences compared with the heavier thallium isotopes. A robust feature in the β-decay pattern of the 7^+ isomer in the heavier thallium isotopes is the feeding of the 8^+ state in the mercury daughter. This is not the case for the decay of ^{180}Tl, because the known 8^+ state in ^{180}Hg [18] is not fed; most of the feeding goes to the 4_1^+ state with feeding of 5^- and 6^+ states. From this it can be deduced that the β-decaying state in ^{180}Tl probably has spin 4 or 5. The coupling of the $3s_{1/2}$ proton to a $1h_{9/2}$ neutron can lead to a 4^- or 5^- state.

The observation in this study of the second 0^+ state and the associated low-spin transitions feeding it is partly due to the feeding through (unobserved) γ-ray transitions. However, it is not clear yet if there is also direct feeding through a possible, but yet unobserved, low-spin state in ^{180}Tl. Nevertheless, the half-life of ^{180}Tl obtained by gating on the 2_1^+ (434 keV) and 2_2^+ (601 keV) transitions in the present work agree with a half-life of $t_{1/2} = 1.09(1)$ s. Hence, based on this experimental fact, no conclusive evidence for the existence of the low-spin isomer in ^{180}Tl has been found. A possibility to settle this issue is expected from a recent in-source laser spectroscopy experiment at ISOLDE where spectra of the decay of ^{180}Tl were taken as a function of the frequency of the ionizing laser light. The analysis of these data is on-going [33].

B. Systematics of even mercury isotopes

In Fig. 1, the newly observed 0_2^+ state at 420 keV, 2_2^+ state at 601 keV, and (2_3^+) state at 1091 keV in ^{180}Hg are shown. The 0_2^+ and 2_2^+ states follow well the general trend established in heavier mercury isotopes and confirm that the minimum of the parabolic behavior in the excitation energy of the prolate band occurs in ^{182}Hg, i.e., at $N = 102$. These two states are the only new energy levels for which a firm spin assignment could be deduced, although it is believed that the state at 1091 keV is

the 2_3^+ state, which according to the systematics is expected to occur around ~ 1 MeV (see Figs. 1 and 10). Furthermore, this state decays to the 0_2^+ and 2_1^+ states via γ decay, so its spin should be 1 or 2. Also, in ^{182,184,186}Hg a similar 2_3^+ state has been observed, which decays similarly only to the 0_2^+ and the 2_1^+ states and not to the ground state (see Fig. 10, the green dotted lines) [20]. This could be an indication that this is the bandhead of the γ vibrational band that is coupled to the prolate band. This assignment is also suggested for the corresponding 2^+ state in ^{184,186}Hg [10,34].

In Fig. 10 the candidates for the 4_2^+ state are also indicated. The 1124 keV level in ^{182}Hg was suggested as a possible candidate for the 4_2^+ level in Ref. [12] and was also observed in Ref. [22,35]. In ^{180}Hg, two possible candidates for the 4_2^+ state are present: the 1203 and 1223 keV levels. The latter is more strongly fed in the β decay of ^{180}Tl, suggesting that if the ground-state spin of ^{180}Tl is indeed (4,5), this would have a higher probability of being the 4_2^+ state. However, by looking at the γ intensities of the transitions originating from these levels and comparing them with those of the 1080 keV level in ^{186}Hg, the 1203 keV level shows closer resemblance to the heavier mercury isotopes, and this would suggest this is the 4_2^+ level in ^{180}Hg.

V. CONCLUSION

The β decay of ^{180}Tl populating levels in ^{180}Hg was studied. As a result, many new low-lying energy states were observed in ^{180}Hg, of which the most significant are the 0_2^+ and 2_2^+ states, at energies of 420 and 601 keV, respectively. They confirm that the minimum of the prolate configuration in the chain of Hg isotopes occurs in ^{182}Hg, i.e., at $N = 102$. Moreover, the possible bandhead of the γ vibrational band built on the prolate deformed state was tentatively identified at 1091 keV.

Furthermore, from the β feeding of the different ^{180}Hg states, the ground-state spin of ^{180}Tl was inferred to be $(4^-,5^-)$. A firmer assignment of the ground-state spin will follow from a hyperfine interaction study [33]. This spin determination and the fact that only one β-decaying isomer is observed in ^{180}Tl is important for the understanding of the β-delayed fission study [19]. The identification of the lowest-energy states and their decays is important for the Coulomb excitation of ^{180}Hg, which has recently become possible. Finally, the ongoing analysis of the data from low-energy Coulomb excitation of $^{182-188}$Hg performed at the radioactive beam experiment (REX) at ISOLDE [13], of the lifetime measurements on $^{184-188}$Hg at the Argonne Tandem-Linac Accelerator System (ATLAS) [36], and of the recent β-decay studies of $^{182-184}$Tl [22] will complement the information on the different structures present in the even-even mercury nuclei near the neutron midshell. With all these observables a full theoretical description comes within reach.

ACKNOWLEDGMENTS

We thank J. L. Wood for fruitful discussions. We thank the ISOLDE Collaboration for providing excellent beams and the GSI Target Group for manufacturing the carbon foils. This work was supported by FWO-Vlaanderen (Belgium), by GOA/2004/03 (BOFK.U.Leuven), by the IUAP–Belgian State Belgian Science Policy (BriX network P6/23), by the European Commission within the Sixth Framework Programme through I3-EURONS (Contract RII3-CT-2004-506065), by the United Kingdom Science and Technology Facilities Council (STFC), and by the Slovak grant agency VEGA (Contract No. 2/0105/11 1/0091/10).

[1] K. Heyde *et al.*, Phys. Rep. **102**, 291 (1983), and references therein.
[2] J. L. Wood *et al.*, Phys. Rep. **215**, 101 (1992), and references therein.
[3] R. Julin *et al.*, J. Phys. G **27**, R109 (2001), and references therein.
[4] J. Bonn *et al.*, Phys. Lett. B **38**, 308 (1972).
[5] T. Kühl, P. Dabkiewicz, C. Duke, H. Fischer, H.-J. Kluge, H. Kremmling, and E.-W. Otten Phys. Rev. Lett. **39**, 180 (1977).
[6] G. Ulm *et al.*, Z. Phys. A **325**, 247 (1986).
[7] D. Proetel *et al.*, Phys. Rev. Lett. **31**, 896 (1973).
[8] N. Rud *et al.*, Phys. Rev. Lett. **31**, 1421 (1973).
[9] J. H. Hamilton *et al.*, Phys. Rev. Lett. **35**, 562 (1975).
[10] J. D. Cole *et al.*, Phys. Rev. Lett. **37**, 1185 (1976).
[11] T. Grahn *et al.*, Phys. Rev. C **80**, 014324 (2009).
[12] M. Scheck *et al.*, Phys. Rev. C **81**, 014310 (2010).
[13] A. Petts *et al.*, in Conference Proceedings CP1090 Capture Gamma-Ray Spectroscopy and Related Topics, 13th International Symposium, 2009 (unpublished), p. 414.
[14] W. Nazarewicz, Phys. Lett. B **305**, 195 (1993).
[15] M. Muikku *et al.*, Phys. Rev. C **58**, R3033 (1998).
[16] M. P. Carpenter *et al.*, Phys. Rev. Lett. **78**, 3650 (1997).
[17] G. D. Dracoulis *et al.*, Phys. Lett. B **208**, 365 (1988).
[18] F. G. Kondev *et al.*, Phys. Rev. C **62**, 044305 (2000).
[19] A. N. Andreyev *et al.*, Phys. Rev. Lett. **105**, 252502 (2010).
[20] Evaluated Nuclear Structure Data File (ENSDF), [http://www.nndc.bnl.gov/ensdf/] .
[21] J. Wauters *et al.*, Phys. Rev. C **50**, 2768 (1994).
[22] E. Rapisarda *et al.* (unpublished).
[23] G. D. Dracoulis, Phys. Rev. C **49**, 3324 (1994).
[24] E. Kugler, Hyperfine Interact. **129**, 23 (2000).
[25] V. N. Fedoseyev *et al.*, Hyperfine Interact. **127**, 409 (2000).
[26] T. J. Giles *et al.*, Nucl. Instr. Meth. B **204**, 497 (2003).
[27] J. Eberth *et al.*, Progr. Part. Nucl. Phys. **46**, 389 (2001).
[28] X-ray Instruments Associates, [http://www.xia.com].
[29] P. Möller, A. J. Sierk1, T. Ichikawa, A. Iwamoto, R. Bengtsson, H. Uhrenholt, and S. Aberg, Phys. Rev. C **79**, 064304 (2009).
[30] T. Kibédi *et al.*, Nucl. Instr. Meth. A **589**, 202 (2008).
[31] J. C. Hardy *et al.*, Phys. Lett. B **71**, 307 (1977).
[32] R. D. Page *et al.*, Phys. Rev. C **84**, 034308 (2011).
[33] V. Liberati *et al.* (unpublished).
[34] J. P. Delaroche *et al.*, Phys. Rev. C **50**, 2332 (1994).
[35] M. Keupers, Master's thesis, University of Leuven, Faculteit Wetenschappen, 2010.
[36] L. Gaffney (unpublished).